Desalination and Water Treatment
www.deswater.com

doi: 10.1080/19443994.2016.1190110

57 (2016) 26670–26679
November

Taylor & Francis
Taylor & Francis Group

Thin-film nanocomposite membrane with vertically embedded carbon nanotube for forward osmosis

Moon Son[a], Vaclav Novotny[a,b], Heechul Choi[a,*]

[a]*School of Environmental Science and Engineering, Gwangju Institute of Science and Technology (GIST), Gwangju 500-712, Republic of Korea, Tel. +82 62 715 2576; Fax: +82 62 715 2434; email: hcchoi@gist.ac.kr (H. Choi)*
[b]*Faculty of Mechanical Engineering, Department of Energy Engineering, Czech Technical University in Prague, Technicka 4, 16607 Prague 6, Czech Republic*

Received 22 December 2015; Accepted 24 December 2015

ABSTRACT

Forward osmosis (FO) for desalination is receiving tremendous attention due to its low energy consumption and simple operation compared to reverse osmosis. Here, we propose a thin-film nanocomposite (TFN) membrane with vertically embedded carbon nanotubes (CNTs) in the active layer to maximize membrane permeability without significantly sacrificing selectivity. We first attempted a spray-assisted electromagnetic field alignment technique to vertically embed CNT in the active layer of the TFN membrane. After vertically embedding the CNT, the developed TFN membrane exhibited 20% increased water flux. When chemical etching of the active layer was further applied, increase in water flux was over 300% (40 LMH). Meanwhile, the increased reverse salt flux was mild most likely due to the steric effect of CNT in the active layer. The developed TFN membrane, thus showed even higher water flux and lower reverse salt flux when compared to recently provided commercial FO membranes. This method is easy to up-scale with a one-step fabrication process, and it is cost-effective due to its simplicity and the low concentration of CNT solution used. Therefore, these findings could contribute to freshwater production using the FO process to overcome global water scarcity.

Keywords: Thin-film nanocomposite; Membrane; Carbon nanotube; Vertically embedded; Forward osmosis

1. Introduction

As water scarcity increases in severity around the world, many countries are struggling to secure freshwater resources [1]. Conventional wastewater treatment and water recycling remain imperfect solutions because regional variation in water resources is worsening due to climate change. For this reason, many consider sea water desalination to be an alternative solution of freshwater supply by utilizing plentiful sea water [2]. Various desalination processes exist, including forward osmosis (FO), reverse osmosis, multi-stage flash, multi-effect distillation, membrane distillation, and capacitive deionization; however, the FO process has drawn attention recently due to its relatively low energy consumption and simple operating conditions [3,4].

*Corresponding author.

Presented at the 8th International Desalination Workshop (IDW) 2015, November 18–21, 2015, Jeju Island, Korea

In FO, the membrane must possess excellent performance. High permeability and selectivity are required to produce the maximum amount of freshwater without simultaneously sacrificing draw solute [5]. The thin-film composite (TFC) membrane, composed of a thin active layer and a porous support layer, is favorable due to its high water flux [6,7]. High permeability membranes, such as polyamide-based TFC membranes, make the FO process commercially reasonable, but there is still room for development. Recently, researchers have aggressively investigated the thin-film nanocomposite (TFN) membrane due to the enhanced permeability induced by the unique properties of nanomaterials [8–28].

Among various nanomaterials, such as carbon nanotube (CNT), zeolite, silica, titania, and alumina, CNT has received the bulk of attention because of its excellent mechanical strength, surface area, hydrophilicity, and alternative pathway for water molecules after functionalization [8–30]. Researchers have thus investigated the TFN membrane with a CNT in the active or support layer [10,31]. Now it has been proven that CNT can accelerate water molecule transport through membranes by providing another pathway inside or on the outer surface of the CNT [32–35]. However, precursor solution filtration or vertically grown array of CNT are required prior to embedding the CNT in the active layer, and a simple method for doing so is needed for commercial viability.

A spray-assisted thin-film formation technique is currently used in layer-by-layer membrane fabrication [36–38]. This technique can homogeneously disperse the CNT on the membrane surface and requires only a tiny amount of precursor solution compared with other methods. Studies have also reported that CNT alignment substantially increases membrane permeability [39,40]; CNT orientation was vertically aligned along the electromagnetic field. Therefore, the membrane could have a vertically embedded CNT in the active layer when the spray-assisted electromagnetic field method is applied.

Based on this rationale, we designed and synthesized a TFN membrane with a vertically embedded CNT in the active layer for the FO process. The performance enhancements in terms of water flux and reverse salt flux were evaluated in a lab-scale FO setup.

2. Material and methods

2.1. Materials

The multi-wall CNT, 10–15 nm in diameter, was supplied by Hanwha Chemical Corporation (CM-150). To functionalize the CNT, nitric acid (ACS reagent, 70%) and sulfuric acid (ACS reagent 95.0–98.0%) were purchased from Sigma–Aldrich. Deionized (DI) water was generated using a water purification system (Synergy, Millipore, USA) and had a resistivity of 18.2 MΩ-cm at room temperature (25˚C). A 0.45 μm nylon filter (Millipore Corporation, USA) and an ultra sonicator (B8510-MT, Branson, USA) were used for uniform dispersion of functionalized CNT (fCNT) and for sieving, respectively.

Polyethersulfone (PES, Solvay Korea Co, Gafone 3000P), with a molecular weight (M_w) of 62,000–64,000 g/mol, was used for support layer fabrication. N-methyl-2-pyrrolidinone (NMP, anhydrous 99.5%, Sigma–Aldrich) and polyvinylpyrrolidone (PVP, M_w: 10,000 g/mol, Sigma–Aldrich) were used as a solvent and pore formation additive, respectively. A casting knife made of high precision-machined iron was also used to obtain constant thickness and surface.

Trimesoyl chloride (TMC, 98%) and m-phenylenediamine (MPD, flakes 99%) were acquired from Sigma–Aldrich to deposit the polyamide (PA) active layer. The n-hexane (anhydrous 95%) and deionized water (DI) water were used as organic and inorganic solvents, respectively. A custom-made acrylic plate was used to hold the membrane during interfacial polymerization (IP), and a commercial rubber roller was used to eliminate the excess amount of solution during the IP process. The NaOCl and $NaHSO_3$ were purchased from Sigma–Aldrich to further modify PA active layer. The electromagnetic field setup to orient the CNT vertically consisted of frame from two steel plates with 50 mm spacing connected to a custom-made 2.5 kV direct current (DC) power supply powered from a regular 220 V power grid.

2.2. PES support layer fabrication

Nonsolvent-induced phase separation (NIPS) was applied to fabricate the support layer of the TFC membrane. PES (17 wt% ratio to total solution) powder was dissolved in the NMP solution with PVP (1 wt% ratio to total solution) to prepare the polymer solution; this solution was immediately sonicated for 3 h and degassed for 30 min to fully remove visible/invisible air bubbles. The prepared polymer solutions were cast onto the glass plate at 100 μm thicknesses using the custom-made casting knife. Afterward, the casted polymer solution was left for 30 s and immersed in the DI water bath for over 30 min. The prepared PES support layer was stored in a bottle of DI water for over 24 h to remove any remaining solvent.

2.3. PA active layer fabrication

Widely used for highly selective PA-based membranes, the IP method was applied to fabricate the PA active layer. The 2 wt% of MPD with 0.5 wt% fCNT in 100 mL DI water was poured onto the support layer's surface. After 2 min, the MPD-saturated membrane was placed in direct contact with 100 mL n-hexane solution containing 0.15 wt% TMC for 2 min. Then, the membrane was cured in an oven at 70˚C for 2 min. The prepared membranes were stored in DI water at 4˚C to remove any unreacted residues.

A custom-made setup for vertical alignment and vertical embedding (VE) of CNT in the PA active layer during IP process of the TFN-VE membrane consisted from a frame holding two steel plates. The plates acted as electrodes as they were connected to an electric potential 2.5 kV DC provided by the custom-made power supply. As illustrated in Fig. 1, the acryl plate holding the support layer was inserted inside this frame to align the CNT in vertical orientation.

The PA active layer in the TFN-VE membrane was chemically etched by NaOCl and $NaHSO_3$, reported and named the TFN-VE500 membrane [28,41]. Table 1 and Fig. 2 provide a summary of the prepared compositions for the synthesized membranes.

2.4. Characterization

Because the opened end-tip of fCNT can allow ultrafast water transport inside it, we conducted transmission electron microscopy (TEM, JEM-2100, Jeol, Japan) analysis to confirm the end-tip of the fCNT were open [32–35]. We investigated the membrane surface and cross-sectional morphology using scanning electron microscopy (SEM, S-4700, Hitachi, Japan). The synthesized membrane was fully dried and cut into a rectangle. Then, we immediately immersed the piece in liquid nitrogen and cracked it to determine the precise cross-sectional structure of the membrane. The types of functional groups on the CNT, fCNT, TFC, and TFN-VE were characterized by Fourier transform infrared spectroscopy (FTIR, 660-IR, Varian, US).

2.5. Lab-scale FO test

We evaluated membrane performance using a lab-scale FO setup in terms of water flux and reverse salt flux (Fig. 3). We used 0.5 M of NaCl aqueous solution and DI water as draw and feed solutions, respectively. As illustrated in Fig. 3, we used a cross-flow membrane test unit, in which the temperature of both draw and feed solutions were controlled at 25 ± 1˚C with a water-cooled chiller (DH-003BH, Daeho Auto Chiller, Korea). Both the draw and feed solutions were circulated with a peristaltic pump (BP-60601, Won Corp., Korea) with a 1,000 cm^3/min cross-flow rate. The effective membrane area of the testing cell was 20 cm^2. We measured the water flux through a mathematic calculation dividing the permeated volume rate by the effective membrane area as follows:

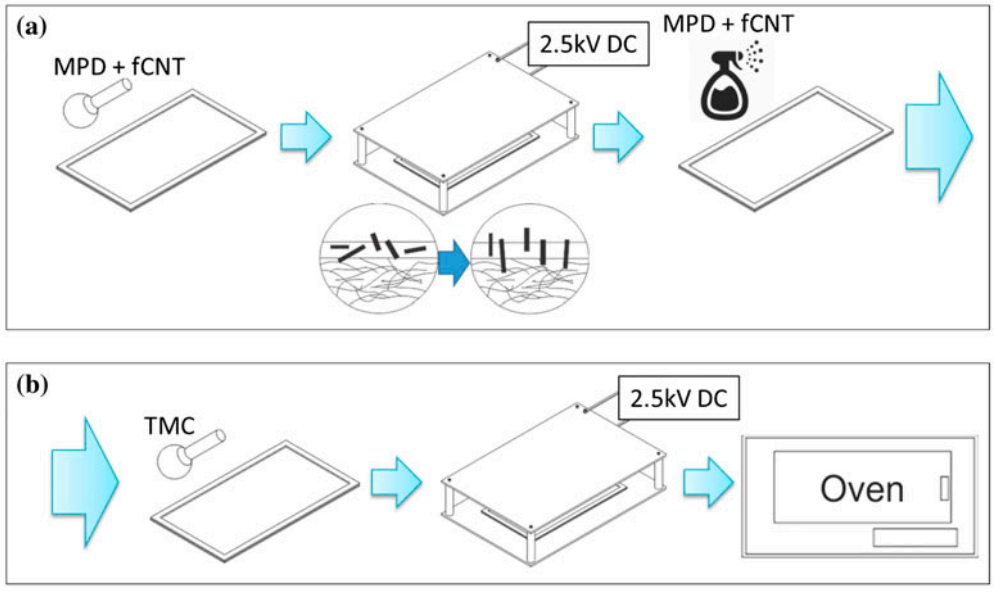

Fig. 1. Schematic illustration of active layer of TFN-VE membrane fabrication processes.

Table 1
Prepared composition of membranes

Classification	TFC	TFN-VE	TFN-VE500
Active layer	Polyamide	Polyamide/fCNT	Etched polyamide/fCNT
Support layer	PES + PVP	PES + PVP	

Notes: Polyamide was etched using NaOCl (500 ppm) and $NaHSO_4$ (1,000 ppm) for TFN-VE500 membrane. TFC: thin-film composite, TFN-VE: thin-film nanocomposite with vertically embedded (VE) CNT in active layer, TFN-VE500: active layer etched TFN-VE, PES: polyethersulfone, PVP: polyvinylpyrrolidone, fCNT: functionalized carbon nanotubes.

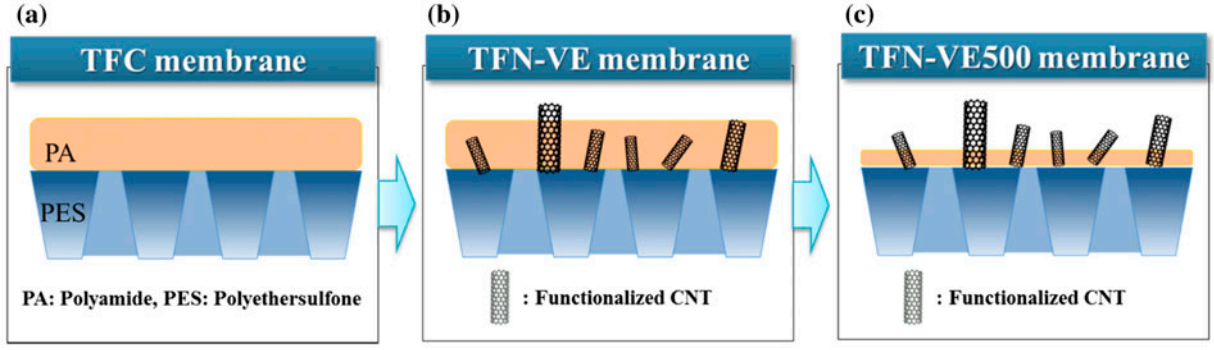

Fig. 2. Structure illustration of prepared: (a) TFC, (b) TFN-VE, and (c) TFN-VE500 membranes.

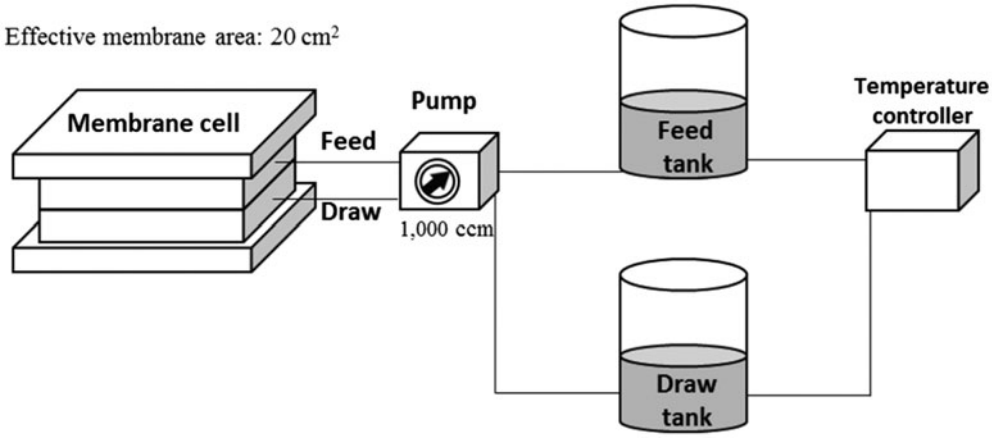

Fig. 3. The lab-scale FO filtration setup.

$$J_W = \frac{V_{FO} - V_F}{A_m t} \quad (1)$$

where J_w is the measured water-permeated flux, V_{FO} is the initial volume of feed solution, V_F is the final volume of feed solution after operation, A_m is the effective membrane area, and t is time. We measured the final concentration of feed solution with an electrical conductivity meter (YSI-85, YSI Incorporated, USA), after operation to determine the reverse salt flux using following equation:

$$J_S = \frac{C_F V_F}{A_m t} \quad (2)$$

where J_S is the measured reverse salt flux, C_F is the final NaCl concentration of the feed solution after operation, V_F is the final volume of the feed solution after operation, A_m is the effective membrane area,

and t is time. The units of water flux and reverse salt flux are $L\,m^{-2}\,h^{-1}$ (LMH) and $g\,m^{-2}\,h^{-1}$ (gMH), respectively. The FO tests were repeated at least two times for accuracy and reproducibility of the results.

3. Results and discussion

3.1. CNT functionalization

As shown in Fig. 4, the TEM observation is consistent with literature reports, suggesting successful functionalization and opened tips [32–35]. The CNT length also shortened to around 500 nm due to strong acid contact with the CNT during oxidation [12,31]. The fCNT, therefore, had the potential to disperse well in the polymer solution for the active layer; it was also trapped well inside the PA layer.

It has been widely reported that hydrophilic functional groups can attach to the fCNT during the functionalization process. FTIR spectrum analysis to determine the functional groups on the fCNT revealed

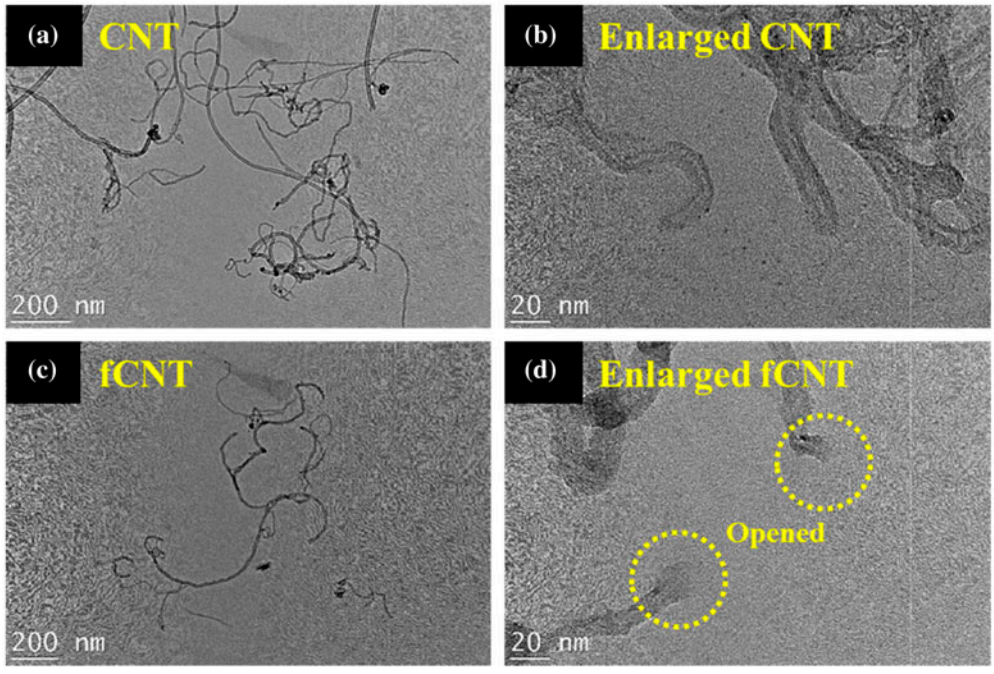

Fig. 4. TEM images of (a–b) CNT and (c–d) fCNT.

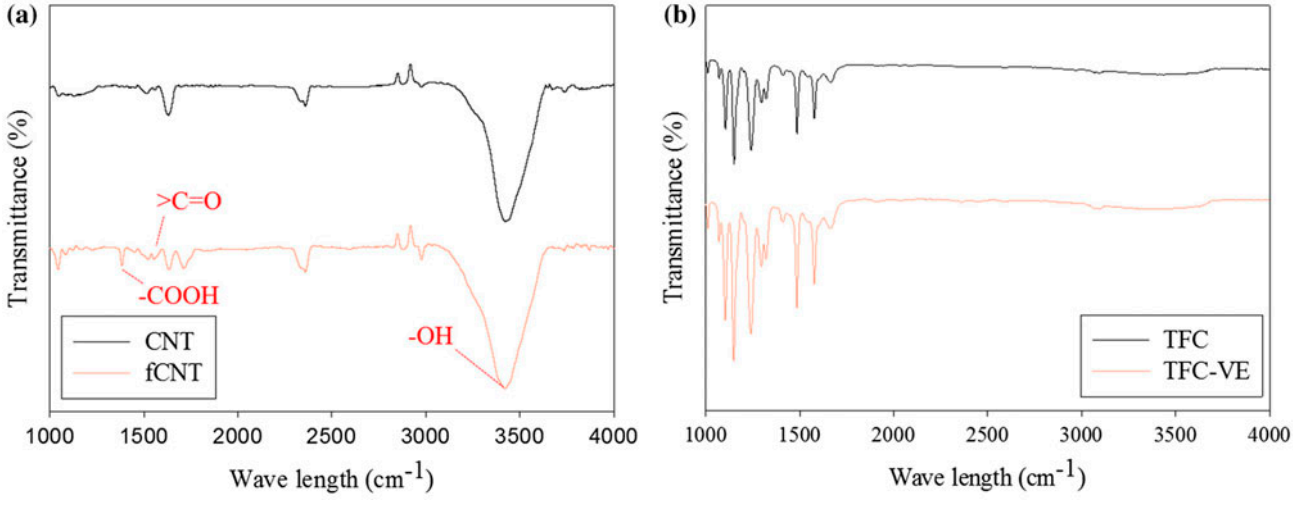

Fig. 5. FTIR spectrum of (a) CNT and fCNT, (b) TFC and TFC-VE membranes.

peaks at 1,380 cm^{-1} (–COOH), 1,547–1,560 cm^{-1} (>C=O), and 3,440 cm^{-1} (–OH) (Fig. 5(a)) [42,43]. Therefore, fCNT has the potential to act as an alternative pathway for water molecules and to increase the hydrophilicity of the membrane, resulting in water-flux enhancement during the FO process.

The FTIR spectra for fully aromatic TMC and 1,3-benzenediamine-based membranes had an amide II band (1,541 cm^{-1}) and an aromatic amide band (1,609 cm^{-1}) that were absent for the semi-aromatic membranes [44]. The peaks of functional groups, such as carboxyl (–COOH), carbonyl (>C=O), and hydroxyl groups (–OH), were hindered by the overlapping effects of the polymer peaks after embedding fCNT in the active layer of the TFC-VE membrane due to the relatively small amount of CNT used (Fig. 5(b)). The functional groups of TFN-VE500 membrane were not investigated because the TFN-VE membrane already possessed fCNT.

3.2. Morphology analysis of prepared membranes

Composed of the PA active layer and PES support layer, the TFN-VE membrane was successfully synthesized. Fig. 6(a)–(b) shows that the PA layer was deposited well with a generic ridge-and-valley structure. In addition, its support layer had uniform finger-like structures, which are favored for FO processes in order to minimize the structure parameters; such

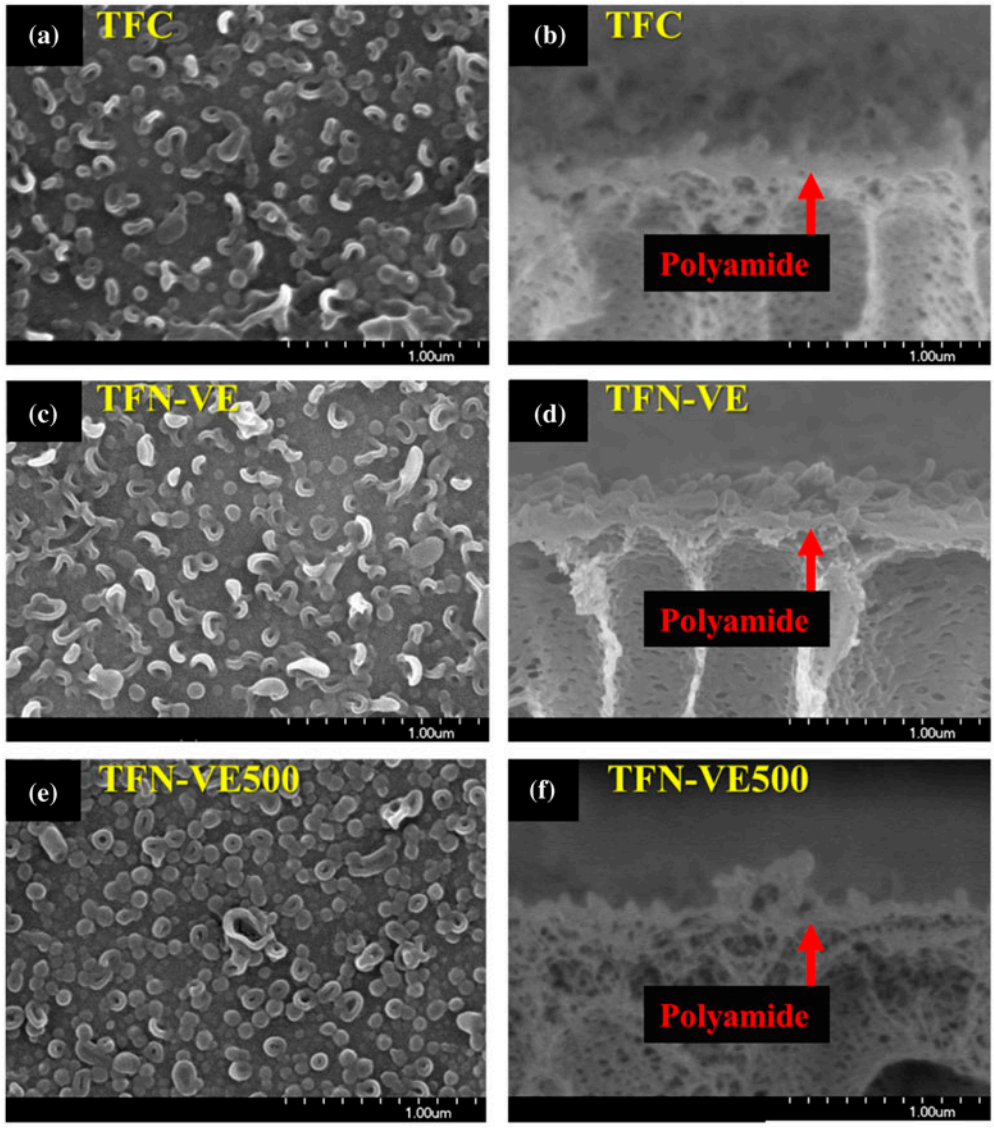

Fig. 6. Surface and cross-sectional SEM images of (a–b) TFC, (c–d) TFN-VE and (e–f) TFN-VE500 membranes.

structures have a tortuosity of near unity (Fig. 6(b), (d) and (f)) [45].

The conventional method with the TFN membrane and CNT in the PA layer requires an additional filtration step with MPD solution, which is not eco-friendly and difficult to scale up for commercialization. Without that additional filtration step, the CNT is immediately washed out of the PA layer during the fabrication step. To overcome these issues, we applied a spray-assisted electromagnetic field method during the fabrication step to make the CNT vertically embedded in the PA matrix. Researchers recently used similar method in the gas filtration membrane to vertically align the CNT in a polymer matrix [39]. It was difficult to detect the presence of fCNT in the PA layer due to the low concentration of fCNT (0.5 wt%) compared to the total MPD solution. There was also a hindering effect due to the structure of the PA layer, as shown in Fig. 6(c)–(f). Nonetheless, the membranes synthesized by either similar electromagnetic (EM) field-based or another method of vertically embedding CNT in the polymer matrix have increased permeability [39,40]. Sharma et al. also reported that CNT were well aligned in polymer matrix (polycarbonate) by applying EM field [39]. When the fCNT concentration is higher than 0.5 wt%, fCNT aggregate each other, and the membrane exhibits poor performance due to the decreased selectivity under the same experimental conditions.

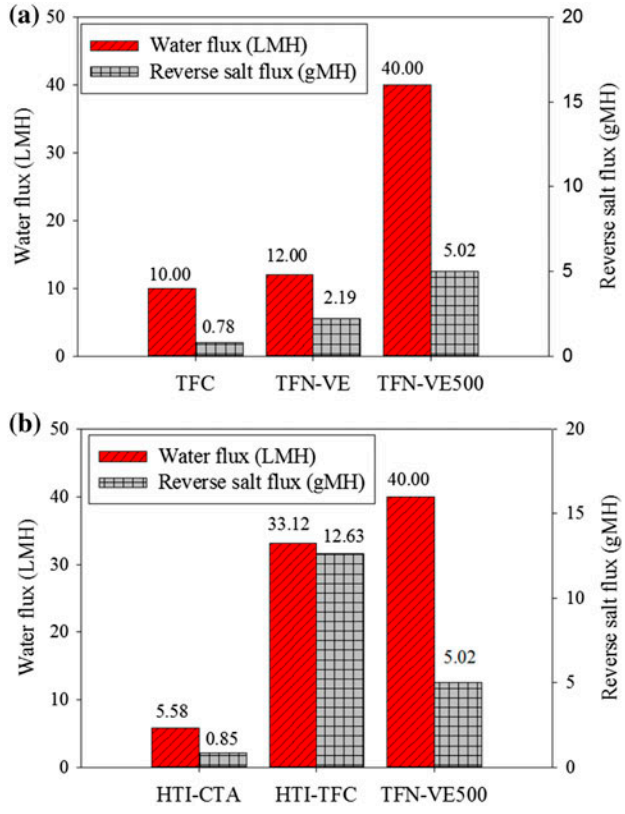

Fig. 7. The water flux and reverse salt flux of (a) TFC, TFN-VE, and TFN-VE500 membranes and (b) HTI-CTA, HTI-TFC, and TFN-VE500 membranes in FO. The 0.5 M NaCl and DI water were used as draw and feed solutions, respectively.

3.3. Membrane performance in FO

The water flux of TFN-VE membrane increased by 20% in the FO, from 10.00 LMH to 12.00 LMH, due to the presence of fCNT in the PA layer compared with the bare TFC membrane (Fig. 7(a)). The reverse salt flux of the TFN-VE membrane, which is one of the representative parameters of membrane selectivity in FO, also increased, from 0.78 to 2.19 gMH, in tandem with increased water flux. This water flux and reverse salt flux incensement indicate that the gap between the CNT and PA layer formed during the IP process; meanwhile, the inner holes of the CNT served as extra pathways allowing water molecules and hydrated salt ions to penetrate the active layer because the CNT used in this study was 10–15 nm in diameter. As illustrated in Fig. 2, vertically aligned CNT can play important role as alternative channel for water molecules and hydrated salt ions resulting in increased the water flux and the reverse salt flux, simultaneously. However, the single-wall CNT did not lead to significant flux enhancement under the same experimental conditions, and the multi-wall CNT has cost benefits. Due to chemical damage in the PA layer compared with the TFN-VE membrane, the water flux of the TFN-VE500 membrane dramatically increased by over 3 times, from 12.00 to 40.00 LMH as shown in Fig. 7(a). Studies have reported that chemical etching of the PA layer significantly increases both water flux and reverse salt flux [28,31,41]. The chemical etching method increased membrane permeability due to not only opening up the end-tips of CNT blocked by PA layer to serve as alternative channel for water molecules, but also due to decreased cross-linking of PA layer as illustrated in Fig. 2(b)–(c) [31,41]. However, compared with the TFN-VE membrane simultaneously, the TFN-VE500 membrane exhibited significantly increased water flux and moderately increased reverse salt flux, from 2.19 to 5.02 gMH. This phenomenon could be interpreted as a steric effect of CNT in the PA layer. CNT is physicochemically stable, and well-scattered CNT prevents damage to the PA layer during the chemical etching step. As expected, the PA layer covering the CNT was etched, allowing CNT to act as an ultrafast pathway. Therefore, the combined effects of CNT resulted in moderately

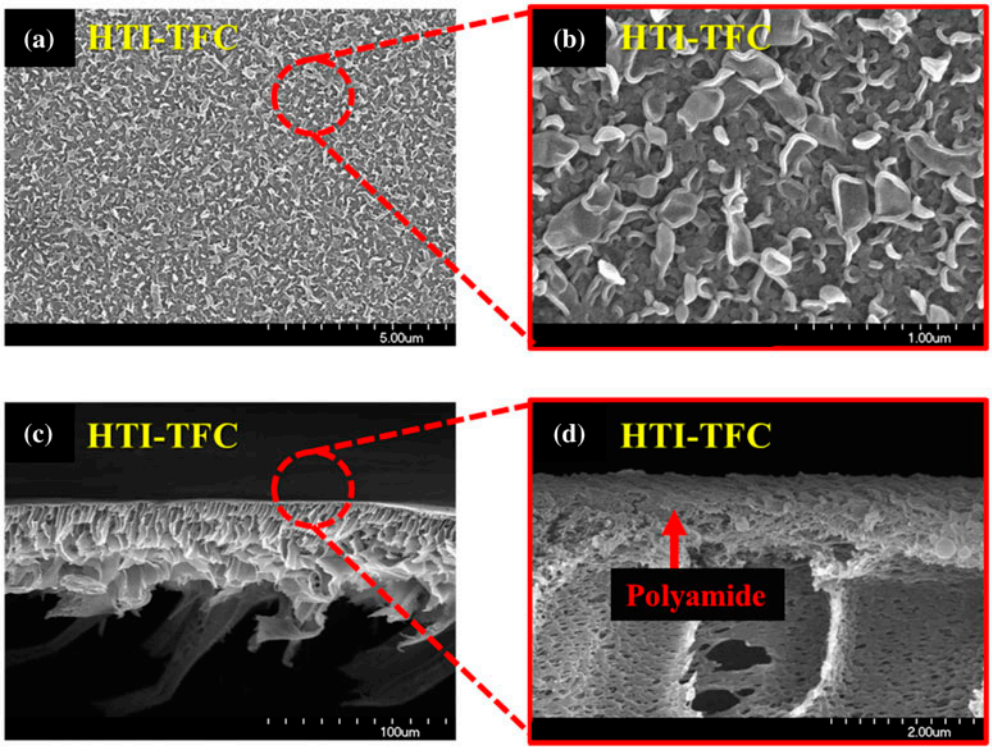

Fig. 8. (a–b) Surface and (c–d) cross-sectional SEM images of commercial HTI-TFC membrane.

increased reverse salt flux, while water flux increased significantly after chemical etching of the PA layer.

Recently, several commercial FO membranes have become available in the market, and HTI Inc. produced a cellulose triacetate (CTA)-based and PA-based FO membrane named HTI-CTA and HTI-TFC membranes, respectively, which were tested under same conditions as previous membranes. Due to the dense structure of the active layer, the HTI-CTA membrane exhibited a relatively low water flux of 5.58 LMH and reverse salt flux of 0.85 gMH. The HTI-TFC membrane is comparable because it is also composed of a polymer support layer and a PA active layer, as shown in Fig. 8. The HTI-TFC membrane showed a high water flux of 33.12 LMH and reverse salt flux of 12.63 gMH because of its favorable thin active layer compared to the HTI-CTA membrane. However, the developed TFN-VE500 membrane exhibited a higher water flux and lower reverse salt flux compared to the HTI-TFC membrane, as shown in Fig. 7(b). With its high water flux and low reverse salt flux, the membrane is promising in FO because it generates more water without losing the draw solute dissolved in the draw solution. Thus, the developed TFN-VE500 membrane has great potential for commercialization due to its excellent performance and easy to up-scale.

4. Conclusions

In this study, we propose a TFN membrane with vertically embedded CNT in the active layer for the FO process. This type of TFN membrane exhibited 20% increased water flux, from 10 to 12 LMH, when CNT was vertically embedded in the PA layer and over three times higher water flux (to 40 LMH) after chemical etching of the active layer. The presence of the CNT in the PA layer prevents chemical damage during the etching step, maximizing the membrane's water flux. Thus, we can take advantage of chemical etching without significantly sacrificing membrane selectivity. Moreover, the developed TFN membrane exhibited even higher water flux and lower reverse salt flux compared with the commercial HTI-TFC membrane, which is one of the most famous FO membranes on the market. This method is easy to up-scale compared with other methods of incorporating the CNT in the PA layer; it is also cost-effective due to the relatively low concentration of CNT used. However, there is still room for steric interpretation of vertically embedded CNT in the PA layer to support these results. These findings could contribute to fresh water production by utilizing the tremendous potential of sea water. We also expect further potential of the

presented method for membrane synthesis in the field of pressure-retarded osmosis for electricity production from saline water.

Acknowledgement

This research was supported by the R&D Program of the Society of the National Research Foundation (NRF) and funded by the Ministry of Science, ICT & Future Planning (Grant Nos.: NRF-2014M3C8A4030498, 2015R1A2A2A10027866, and 2014K000274) and partially by the "Basic Research Projects in High-tech Industrial Technology" project through a grant provided by GIST in 2015.

References

[1] M. Son, H. Choi, L. Liu, H. Park, H. Choi, Optimized synthesis conditions of polyethersulfone support layer for enhanced water flux for thin film composite membrane, Environ. Eng. Res. 19 (2014) 339–344.
[2] M. Elimelech, W.A. Phillip, The future of seawater desalination: Energy, technology, and the environment, Science 333 (2011) 712–717.
[3] D.L. Shaffer, J.R. Werber, H. Jaramillo, S. Lin, M. Elimelech, Forward osmosis: Where are we now? Desalination 356 (2015) 271–284.
[4] Y. Sato, S. Nakao, Theoretical estimation of semi-permeable membranes leading to development of forward osmosis membranes and processes as a future seawater desalination technology, Desalin. Water Treat. 57(12) (2014) 5398–5405.
[5] H. Choi, M. Son, S. Yoon, E. Celik, S. Kang, H. Park, C.H. Park, H. Choi, Alginate fouling reduction of functionalized carbon nanotube blended cellulose acetate membrane in forward osmosis, Chemosphere 136 (2015) 204–210.
[6] C. Klaysom, T.Y. Cath, T. Depuydt, I.F.J. Vankelecom, Forward and pressure retarded osmosis: Potential solutions for global challenges in energy and water supply, Chem. Soc. Rev. 42 (2013) 6959–6989.
[7] N.Y. Yip, A. Tiraferri, W.A. Phillip, J.D. Schiffman, L.A. Hoover, Y. Kim, M. Elimelech, Thin-film composite pressure retarded osmosis membranes for sustainable power generation from salinity gradients, Environ. Sci. Technol. 45 (2011) 4360–4369.
[8] B.-H. Jeong, E.M.V. Hoek, Y. Yan, A. Subramani, X. Huang, G. Hurwitz, A.K. Ghosh, A. Jawor, Interfacial polymerization of thin film nanocomposites: A new concept for reverse osmosis membranes, J. Membr. Sci. 294 (2007) 1–7.
[9] M. Amini, M. Jahanshahi, A. Rahimpour, Synthesis of novel thin film nanocomposite (TFN) forward osmosis membranes using functionalized multi-walled carbon nanotubes, J. Membr. Sci. 435 (2013) 233–241.
[10] H. Kim, K. Choi, Y. Baek, D. Kim, J. Shim, J. Yoon, J.-C. Lee, High-performance reverse osmosis cnt/polyamide nanocomposite membrane by controlled interfacial interactions, ACS Appl. Mater. Interfaces 6 (2014) 2819–2829.
[11] H. Zhao, S. Qiu, L. Wu, L. Zhang, H. Chen, C. Gao, Improving the performance of polyamide reverse osmosis membrane by incorporation of modified multi-walled carbon nanotubes, J. Membr. Sci. 450 (2014) 249–256.
[12] M. Son, H. Choi, L. Liu, E. Celik, H. Park, H. Choi, Efficacy of carbon nanotube positioning in the polyethersulfone support layer on the performance of thin-film composite membrane for desalination, Chem. Eng. J. 266 (2015) 376–384.
[13] C. Lannoy, D. Jassby, K. Gloe, A.D. Gordon, M.R. Wiesner, Aquatic biofouling prevention by electrically charged nanocomposite polymer thin film membranes, Environ. Sci. Technol. 47 (2013) 2760–2768.
[14] L. Zhang, G. Shi, S. Qiu, L. Cheng, H.-L. Chen, Preparation of high-flux thin film nanocomposite reverse osmosis membranes by incorporating functionalized multi-walled carbon nanotubes, Desalin. Water Treat. 34 (2011) 19–24.
[15] J. Park, W. Choi, S. Kim, B. Chun, J. Bang, K.B. Lee, Enhancement of chlorine resistance in carbon nanotube based nanocomposite reverse osmosis membranes, Desalin. Water Treat. 15 (2010) 198–204.
[16] M.T.M. Pendergast, J.M. Nygaard, A.K. Ghosh, E.M.V. Hoek, Using nanocomposite materials technology to understand and control reverse osmosis membrane compaction, Desalination 261 (2010) 255–263.
[17] J. Yin, E.S. Kim, J. Yang, B. Deng, Fabrication of a novel thin-film nanocomposite (TFN) membrane containing MCM-41 silica nanoparticles (NPs) for water purification, J. Membr. Sci. 423–424 (2012) 238–246.
[18] G.L. Jadav, V.K. Aswal, P.S. Singh, SANS study to probe nanoparticle dispersion in nanocomposite membranes of aromatic polyamide and functionalized silica nanoparticles, J. Colloid Interface Sci. 351 (2010) 304–314.
[19] G.L. Jadav, P.S. Singh, Synthesis of novel silica-polyamide nanocomposite membrane with enhanced properties, J. Membr. Sci. 328 (2009) 257–267.
[20] D. Emadzadeh, W.J. Lau, T. Matsuura, A.F. Ismail, M. Rahbari-Sisakht, Synthesis and characterization of thin film nanocomposite forward osmosis membrane with hydrophilic nanocomposite support to reduce internal concentration polarization, J. Membr. Sci. 449 (2014) 74–85.
[21] D. Emadzadeh, W.J. Lau, A.F. Ismail, Synthesis of thin film nanocomposite forward osmosis membrane with enhancement in water flux without sacrificing salt rejection, Desalination 330 (2013) 90–99.
[22] B. Rajaeian, A. Rahimpour, M.O. Tade, S. Liu, Fabrication and characterization of polyamide thin film nanocomposite (TFN) nanofiltration membrane impregnated with TiO_2 nanoparticles, Desalination 313 (2013) 176–188.
[23] E.S. Kim, G. Hwang, M. Gamal El-Din, Y. Liu, Development of nanosilver and multi-walled carbon nanotubes thin-film nanocomposite membrane for enhanced water treatment, J. Membr. Sci. 394–395 (2012) 37–48.
[24] H. Huang, X. Qu, H. Dong, L. Zhang, H. Chen, Role of NaA zeolites in the interfacial polymerization process towards a polyamide nanocomposite reverse osmosis membrane, RSC Adv. 3 (2013) 8203–8207.

[25] H. Huang, X. Qu, X. Ji, X. Gao, L. Zhang, H. Chen, L. Hou, Acid and multivalent ion resistance of thin film nanocomposite RO membranes loaded with silicalite-1 nanozeolites, J. Mater. Chem. A 1 (2013) 11343–11349.
[26] M. Lind, D. Suk, T.V. Nguyen, E.M.V. Hoek, Tailoring the structure of thin film nanocomposite membranes to achieve seawater ro membrane performance, Environ. Sci. Technol. 44 (2010) 8230–8235.
[27] M. Lind, B. Jeong, A. Subramani, X. Huang, E.M.V. Hoek, Effect of mobile cation on zeolite-polyamide thin film nanocomposite membranes, J. Mater. Res. 24 (2009) 1624–1631.
[28] X. Song, Z. Liu, D.D. Sun, Energy recovery from concentrated seawater brine by thin-film nanofiber composite pressure retarded osmosis membranes with high power density, Energy Environ. Sci. 6 (2013) 1199–1210.
[29] E. Celik, L. Liu, H. Choi, Protein fouling behavior of carbon nanotube/polyethersulfone composite membranes during water filtration, Water Res. 45 (2011) 5287–5294.
[30] E. Celik, H. Park, H. Choi, H. Choi, Carbon nanotube blended polyethersulfone membranes for fouling control in water treatment, Water Res. 45 (2011) 274–282.
[31] M. Son, H. Park, L. Liu, H. Choi, J.H. Kim, H. Choi, Thin-film nanocomposite membrane with CNT positioning in support layer for energy harvesting from saline water, Chem. Eng. J. 284 (2016) 68–77.
[32] K. Falk, F. Sedlmeier, L. Joly, R.R. Netz, L.r. Bocquet, Molecular origin of fast water transport in carbon nanotube membranes: Superlubricity versus curvature dependent friction, Nano Lett. 10 (2010) 4067–4073.
[33] J.A. Thomas, A.J.H. McGaughey, Reassessing fast water transport through carbon nanotubes, Nano Lett. 8 (2008) 2788–2793.
[34] J.K. Holt, H.G. Park, Y. Wang, M. Stadermann, A.B. Artyukhin, C.P. Grigoropoulos, A. Noy, O. Bakajin, Fast mass transport through sub-2-nanometer carbon nanotubes, Science 312 (2006) 1034–1037.
[35] A. Kalra, S. Garde, G. Hummer, Osmotic water transport through carbon nanotube membranes, Proc. Natl. Acad. Sci. 100 (2003) 10175–10180.
[36] L. Liu, M. Son, H. Park, E. Celik, C. Bhattacharjee, H. Choi, Efficacy of CNT-bound polyelectrolyte membrane by spray-assisted layer-by-layer (LbL) technique on water purification, RSC Adv. 4 (2014) 32858–32865.
[37] L. Liu, D.Y.W. Di, H. Park, M. Son, H. Hur, H. Choi, Improved antifouling performance of polyethersulfone (PES) membrane via surface modification by CNTs bound polyelectrolyte multilayers, RSC Adv. 5 (2015) 7340–7348.
[38] L. Liu, M. Son, S. Chakraborty, C. Bhattacharjee, H. Choi, Fabrication of ultra-thin polyelectrolyte/carbon nanotube membrane by spray-assisted layer-by-layer technique: Characterization and its anti-protein fouling properties for water treatment, Desalin. Water Treat. 51 (2013) 6194–6200.
[39] A. Sharma, S. Kumar, B. Tripathi, M. Singh, Y.K. Vijay, Aligned CNT/Polymer nanocomposite membranes for hydrogen separation, Int. J. Hydrogen Energy 34 (2009) 3977–3982.
[40] S. Kim, J.R. Jinschek, H. Chen, D.S. Sholl, E. Marand, Scalable fabrication of carbon nanotube/polymer nanocomposite membranes for high flux gas transport, Nano Lett. 7 (2007) 2806–2811.
[41] G. Han, S. Zhang, X. Li, T.S. Chung, High performance thin film composite pressure retarded osmosis (PRO) membranes for renewable salinity-gradient energy generation, J. Membr. Sci. 440 (2013) 108–121.
[42] S. Kang, B. Xing, Adsorption of dicarboxylic acids by clay minerals as examined by in Situ ATR-FTIR and ex Situ DRIFT, Langmuir 23 (2007) 7024–7031.
[43] U.J. Kim, C.A. Furtado, X. Liu, G. Chen, P.C. Eklund, Raman and IR spectroscopy of chemically processed single-walled carbon nanotubes, J. Am. Chem. Soc. 127 (2005) 15437–15445.
[44] V. Freger, J. Gilron, S. Belfer, TFC polyamide membranes modified by grafting of hydrophilic polymers: An FT-IR/AFM/TEM study, J. Membr. Sci. 209 (2002) 283–292.
[45] J. Wei, C. Qiu, C.Y. Tang, R. Wang, A.G. Fane, Synthesis and characterization of flat-sheet thin film composite forward osmosis membranes, J. Membr. Sci. 372 (2011) 292–302.